

Citation: Bellucci, J. and Nemchin, A. and Whitehouse, M. and Snape, J. and Bland, P. and Benedix, G. and Roszjar, J. 2018. Pb evolution in the Martian mantle. *Earth and Planetary Science Letters*. 485: pp. 79-87. <http://doi.org/10.1016/j.epsl.2017.12.039>

## 1 Pb evolution in the Martian mantle

2 J. J. Bellucci<sup>1\*</sup>, A. A. Nemchin<sup>1,2</sup>, M. J. Whitehouse<sup>1</sup>, J. F. Snape<sup>1</sup>, P. Bland<sup>2</sup>, G.K.  
3 Benedix<sup>2</sup>, J. Roszjar<sup>3</sup>

4

5 \*Corresponding author, email address: [jeremy.bellucci@gmail.com](mailto:jeremy.bellucci@gmail.com)

6

7 <sup>1</sup>Department of Geosciences, Swedish Museum of Natural History, SE-104 05  
8 Stockholm, Sweden

9 <sup>2</sup> Department of Applied Geology, Curtin University, Perth, WA 6845, Australia

10 <sup>3</sup>Department of Mineralogy and Petrography, Natural History Museum Vienna, Burgring  
11 7, 1010 Vienna, Austria.

12

## 13 **Abstract**

14 The initial Pb compositions of one enriched shergottite, one intermediate  
15 shergottite, two depleted shergottites, and Nakhla have been measured by Secondary Ion  
16 Mass Spectrometry (SIMS). These values, in addition to data from previous studies using  
17 an identical analytical method performed on three enriched shergottites, ALH 84001, and  
18 Chassigny, are used to construct a unified and internally consistent model for the  
19 differentiation history of the Martian mantle and crystallization ages for Martian  
20 meteorites is presented. The differentiation history of the shergottites and  
21 Nakhla/Chassigny are fundamentally different, which is in agreement with short-lived  
22 radiogenic isotope systematics. The initial Pb compositions of Nakhla/Chassigny are best  
23 explained by late addition of a Pb-enriched component with a primitive, non-radiogenic  
24 composition. In contrast, the Pb isotopic compositions of the shergottite group indicate a  
25 relatively simple evolutionary history of the Martian mantle that can be modeled based  
26 on recent results from the Sm-Nd system. The shergottites have been linked to a single  
27 mantle differentiation event at 4504 Ma. Thus, the shergottite Pb isotopic model here  
28 reflects a two-stage history 1) pre-silicate differentiation (4504 Ma) and 2) post-silicate  
29 differentiation to the age of eruption (as determined by concordant radiogenic isochron  
30 ages). The  $\mu$ -values ( $^{238}\text{U}/^{204}\text{Pb}$ ) obtained for these two different stages of Pb growth are  
31  $\mu_1$  of 1.8 and a range of  $\mu_2$  from 1.4 - 4.7, respectively. The  $\mu_1$ -value of 1.8 is in broad  
32 agreement with enstatite and ordinary chondrites and that proposed for proto Earth,  
33 suggesting this is the initial  $\mu$ -value for inner Solar System bodies. When plotted against  
34 other source radiogenic isotopic variables ( $\text{Sr}_i$ ,  $\gamma^{187}\text{Os}$ ,  $\epsilon^{143}\text{Nd}$ , and  $\epsilon^{176}\text{Hf}$ ), the second  
35 stage mantle evolution range in observed mantle  $\mu$ -values display excellent linear  
36 correlations ( $r^2 > 0.85$ ) and represent a spectrum of Martian mantle mixing-end members  
37 (depleted, intermediate, enriched).

38

39

40

41

42

43 **1. Introduction**

44

45 The Pb isotopic system, which contains the daughter products of three long-lived  
46 decay chains of  $^{238}\text{U}$ ,  $^{235}\text{U}$ , and  $^{232}\text{Th}$ , has been invaluable in constraining the evolution  
47 and differentiation history of the Earth's mantle, crust, core, the lunar mantle, and the  
48 formation of the Earth-Moon system (e.g., Stacey and Kramers, 1975, Zartman and  
49 Haines, 1988, Hart et al., 1992, Connelly and Bizzarro, 2016, Snape et al., 2016). For  
50 Mars, however, there has been significant difficulty in applying this isotopic system due  
51 to the fact that Mars has a mantle with low  $\mu$ -values ( $^{238}\text{U}/^{204}\text{Pb}$ ) that range from 1-5  
52 (Nakamura et al., 1982, Chen and Wasserburg, 1986, Jagoutz, 1991, Borg et al., 2005,  
53 Gaffney et al., 2007, Bouvier et al., 2008, 2009, Bellucci et al., 2015a). Rocks derived  
54 from long-lived, low  $\mu$  reservoirs that have even minor contamination from materials  
55 derived from higher  $\mu$  reservoirs such as the Martian or Earth's crusts ( $\mu$ -values of 14  
56 and 8-10, respectively; Stacey and Kramers, 1975, Bellucci et al., 2015b) will then  
57 produce ambiguous, linear trends in Pb isotopic diagrams. These linear trends, if  
58 interpreted incorrectly could be used to define  $>4$  Ga crystallization ages for relatively  
59 recent rocks (Gaffney et al., 2007, Bouvier et al., 2008, 2009, Bellucci et al., 2016).  
60 Therefore, in cases where mixing between unradiogenic and radiogenic reservoirs may  
61 have occurred, particularly at the scale of individual minerals in Martian meteorites (e.g.,  
62 Bellucci et al., 2016), the best approach to obtain any reliable information is to try and  
63 constrain the mixing end-members present in a single sample. For Martian samples, these  
64 mixing end-members are: 1) initial Pb, present at the time of a rock's crystallization, 2)

65 radiogenic Pb, from the decay of U or Th present in some minerals since the time of  
66 crystallization, and 3) any un-supported radiogenic Pb inherited either from residence and  
67 mixing with radiogenic reservoir(s) on the Martian surface or terrestrial contamination  
68 (e.g., Gaffney et al., 2007, Bellucci et al., 2016).

69 One approach to constrain these mixing end-members is to apply an *in situ*  
70 analytical technique such as Secondary Ion Mass Spectrometry (SIMS) to target  
71 individual minerals in a given rock. This technique has the distinct advantage of  
72 minimizing any crystal boundary/surface contamination by targeting the centers of  
73 crystals, while at the same time avoiding U-bearing inclusions. Although individual  
74 measurements may be relatively imprecise, this method can produce large, statistically  
75 significant data sets with invaluable spatial and mineralogical context. Assuming that a  
76 large, statistically identical group can represent each individual mixing end-member  
77 confidently, this approach has been able to identify the most unradiogenic Pb in several  
78 Martian meteorites, which was interpreted as an accurate representation of initial Pb  
79 values (Bellucci et al., 2015a, 2016). Initial Pb is preserved in minerals that have an  
80 extremely low U/Pb or Th/Pb and have no radiogenic Pb ingrowth. Therefore, initial Pb  
81 can be used to define time integrated chemical variables  $\mu$  and  $\kappa$  ( $= {}^{232}\text{Th}/{}^{238}\text{U}$ ) of a  
82 sample's source and define a Pb model age based on a model of Pb growth in the host  
83 planetary body. This approach has been used successfully to constrain the Pb evolution in  
84 the mantles of the Earth, the Moon, and Mars (Stacey and Kramers, 1975, Bellucci et al.,  
85 2015a, Connelly and Bizzarro, 2016, Snape et al., 2016). While these models of Pb  
86 growth are almost certainly not accurate representations of the complex processes  
87 involved in planetary evolution, they provide useful first order mathematical

88 quantifications of invaluable geochemical variables ( $\mu$  and  $\kappa$ ) in different reservoirs on a  
89 planetary body.

90 While none of the known Martian meteorites are thought to come directly from  
91 the Martian mantle, several varieties are mafic- to ultramafic rocks that are mantle  
92 derivatives. These include the shergottites, nakhlites, and chassignites (collectively the  
93 SNCs), Allan Hills (ALH) 84001, and a unique type of augite-rich shergottite, Northwest  
94 Africa (NWA) 8195. The shergottites can be classified based on their bulk rock rare earth  
95 element (REE) patterns including enriched (flat-slightly depleted REE), intermediate  
96 (slightly depleted LREE), and depleted (strongly depleted LREE) (e.g., Borg et al., 1997,  
97 2003, 2005, Borg and Draper 2003). Based on the combined isotopic systems of Lu-Hf,  
98 Sm-Nd and U-Pb, the differentiation history of the source reservoirs of ALH 84001 and  
99 the shergottites can be linked with a single mantle differentiation event (Lapen et al.,  
100 2010, Bellucci et al., 2015a, Borg et al., 2016, Kruijer et al., 2017). The most recent and  
101 comprehensive  $^{146}\text{Sm}$ - $^{142}\text{Nd}$  and  $^{147}\text{Sm}$ - $^{143}\text{Nd}$  isotopic study indicates this event likely  
102 occurred at  $4504^{+5.4}_{-5.7}$  Ma (Borg et al., 2016). In contrast, the  $^{146}\text{Sm}$ - $^{142}\text{Nd}$  and  $^{182}\text{Hf}$ -  
103  $^{182}\text{W}$  systems indicate that the mantle differentiation histories for the shergottites must be  
104 fundamentally different from that of the nakhlites and chassignites (Kleine et al., 2004,  
105 2009, Foley et al., 2005, Nimmo and Kleine, 2007, Dauphas and Pourmand, 2011,  
106 Mezger et al., 2013). The difference in  $^{142}\text{Nd}$  compositions between the meteorite groups  
107 has been attributed to a mantle overturn early in Martian history (Debaille et al., 2009)  
108 Alternatively, the difference in  $\epsilon^{182}\text{W}$  between the shergottites and nakhlites/chassignites  
109 has been explained by the late addition(s) of material to the Martian mantle. There are  
110 currently two scenarios that can account for the late addition(s) to the Nakhla/Chassigny

111 source, which are: 1) protracted accretion producing variable amounts of  $^{182}\text{W}$  measured  
112 in the Martian meteorite groups ( $\epsilon^{182}\text{W}$  of -0.7 vs 3) or 2) rapid cooling of a planetary  
113 embryo and then a distinct later addition by a significant impactor melting a major  
114 portion of the mantle (e.g., Metzger et al., 2013, Borg et al., 2016). Regardless of the  
115 actual scenario of mantle accretion/differentiation that took place leading to the different  
116  $\epsilon^{182}\text{W}$  compositions of the shergottites and the nakhlites/chassignites, two important  
117 conclusions can be made: 1) there were very likely late additions of primitive  
118 composition to the Martian mantle and 2) it is likely that core formation occurred rapidly,  
119 with the average estimate of age of core formation at  $4559 \pm 8$  Ma ( $2\sigma$ , which is the  
120 average of all core-formation ages reported in Kleine et al., 2004, 2009, Foley et al.,  
121 2005, Nimmo and Kleine, 2007, Dauphas and Pourmand, 2011). The aim of this study is  
122 to obtain the initial Pb composition of at least one of each variety of shergottite, Nakhla,  
123 and Chassigny to better constrain the Pb isotopic growth in the Martian mantle.  
124 Importantly, the samples specifically targeted here have well-determined, concordant  
125 ages from several, non-Pb radiogenic, isotopic systems, avoiding the potential  
126 complications listed above. This approach will add new parameters for the differentiation  
127 history of the Martian mantle, investigate the effects of late accretion on Mars through  
128 time-integrated Pb modeling, and define mantle compositional mixing end-members in  
129 terms of  $\mu$ - and  $\kappa$ -values. Subsequently, these models will be used to investigate two un-  
130 dated shergottites to test the applicability of common Pb chronology and source reservoir  
131 composition calculations on samples with unknown ages.

132

## 133 **2. Samples**

134 The studied samples encompass four enriched shergottites (Larkman Nunatak  
135 (LAR) 12011, Ksar Ghilane (KG) 002, Roberts Massif (RBT) 04261 and Zagami), one  
136 intermediate shergottite (ALH 77005), two depleted shergottites (LAR 12095 and  
137 Tissint), the orthopyroxenite ALH 84001, Nahkla, and Chassigny. Sample descriptions  
138 for the previously reported enriched shergottite Pb data and ALH 84001 are available in  
139 Bellucci et al. (2015a) and the sample description and data for Chassigny are available in  
140 Bellucci et al. (2016). Sample descriptions for the samples analyzed in this study are  
141 presented below.

142 For this study one additional enriched shergottite - KG 002 (previously described  
143 by Llorca et al. 2013) has been analyzed. It is a coarse-grained basaltic shergottite with  
144 large grains of maskelynitized plagioclase that are 4 to 5 mm in size. KG 002 has a REE  
145 pattern that is slightly depleted in LREE and a positive Eu anomaly. The trace element  
146 pattern, major element concentrations, mineral chemistry and petrography are similar to  
147 the enriched shergottite Los Angeles. The cosmic ray exposure age of KG 002 is 3 Ma  
148 but no radiogenic isotopic isochrons are available for this sample to determine the age of  
149 crystallization. As a group, the enriched shergottites have a relatively restricted range in  
150 source reservoir compositions in  $\epsilon^{176}\text{Hf}$  (-17 to -18),  $\epsilon^{143}\text{Nd}$  (-7.2 to -6.7), and  $\gamma^{187}\text{Os}$  (5 to  
151 14.7) (Table 1. Blichert-Toft et al., 1999, Borg et al., 2005, Debaille et al., 2008, Lapen et  
152 al., 2008, Shafer et al., 2010, Brandon et al., 2012, Righter et al., 2015).

153 The intermediate shergottite analyzed for this study, ALH 77005, was originally  
154 described by McSween et al. (1979). Allan Hills 77005 is a cumulate gabbroic rock,  
155 which has had all of its plagioclase converted into maskelynite, and has a slightly  
156 depleted LREE signature. Concordant Rb-Sr and Sm-Nd dates indicate an age of

157 crystallization of  $176 \pm 6$  Ma (Figure 1, Borg et al., 2002). Allan Hills 77005 has a source  
158 reservoir composition in  $\epsilon^{176}\text{Hf}$ ,  $\epsilon^{143}\text{Nd}$ , and  $\gamma^{187}\text{Os}$  of 32.4, 11.1, and 2.1, respectively  
159 (Table 1. Bilchert-Toft et al., 1999, Borg et al., 2002, and Brandon et al., 2012).

160         The two depleted shergottites analyzed for this study were Tissint and LAR  
161 12095. Tissint, described in detail by Balta et al. (2015), has a depleted REE pattern.  
162 Plagioclase has been converted to maskelynite. Tissint also has accessory pyrrhotite that  
163 is suitable for analysis. Additionally, Tissint contains no evidence for terrestrial  
164 alteration, consistent with its recent fall and extremely short residence time in an arid  
165 desert. Ages constrained from Rb-Sr and Sm-Nd isochrons are concordant and have an  
166 average age of  $574 \pm 20$  Ma (Figure 1, Brennecka et al., 2014). Despite the lack of  
167 evidence for terrestrial alteration, Tissint contains multiple sources of Pb and distinct Pb  
168 isotopic compositions from multiple leaching steps (Moriwaki et al., 2017). These  
169 multiple compositions have been interpreted to be remnants of interactions with the  
170 Martian crust (Moriwaki et al., 2017) and thus, *in situ* techniques are likely to be  
171 extremely helpful to obtain the most accurate initial Pb composition possible. Larkman  
172 Nunatak 12095 is a depleted shergottite with an even more depleted LREE pattern than  
173 Tissint (Castle and Herd, 2015). There is no precise chronological information available  
174 for LAR 12095 but a model age, based on Lu-Hf and Sm-Nd isotopic systematics, is  
175 thought to be similar to that of the other depleted shergottites and ranges from 400-550  
176 Ma (Righter et al., 2015). The source reservoir for the depleted shergottites has an  
177 inferred range of  $\epsilon^{176}\text{Hf}$  and  $\epsilon^{143}\text{Nd}$  of 50-58 and 39-42, respectively (Table 1. Grosshans  
178 et al., 2013, Brennecka et al., 2014, Righter et al., 2015).

179 Nakhla is a meteorite fall and terrestrial contamination is assumed to be  
180 negligible. The meteorite is a clinopyroxenite, mainly composed of clinopyroxene with  
181 minor olivine, plagioclase, mesostasis, K-feldspar, oxides, FeS, and chalcopyrite (e.g.,  
182 Harvey and McSween, 1992). Previous studies using a variety of analytical techniques  
183 have obtained a similar crystallization age for Nakhla with an average of  $1362 \pm 54$  Ma  
184 (Figure 1; Papanastassiou and Wasserburg, 1974, Gale et al., 1975, Nakumuru et al.,  
185 1982, Beard et al., 2013). Nakhla has a similar  $\epsilon^{142}\text{Nd}$  signature to that of the depleted  
186 shergottites and Chassigny (Borg et al., 2006, Debaille et al., 2009). However, as stated  
187 above Nakhla and Chassigny are derived from a completely different source reservoir(s)  
188 than that of the shergottites (Debaille et al., 2009, Kleine et al., 2004, 2009, Foley et al.,  
189 2005, Nimmo and Kleine, 2007, Dauphas and Pourmand, 2011). Lastly, Nakhla and  
190 Chassigny have similar ages and source reservoir  $\epsilon^{143}\text{Nd}$  and  $\gamma^{187}\text{Os}$  compositions of 16  
191 and -5.5, respectively (Table 1. Brandon et al., 2000, Misawa et al., 2005, Debaille et al.,  
192 2009).

193

### 194 **3. Analytical Methods**

195 The Pb isotopic compositions of maskelynite, K-feldspar, and/or sulfide grains  
196 were determined using SIMS on polished epoxy-mounted samples or thin sections of  
197 each sample. Before analysis, each sample was cleaned in alternating 1-minute ultrasonic  
198 baths of water and ethanol. After thorough washing, a 30 nm coating of Au was applied  
199 to the surface. All measurements were conducted using a CAMECA IMS1280 instrument  
200 at the Swedish Museum of Natural History, Stockholm (NordSIMS facility) using  
201 previously described experimental protocols (Whitehouse et al., 2005, Bellucci et al.,



202 2015a,b, 2016, Snape et al., 2016). An area of  $35 \times 35 \mu\text{m}$  was rastered for 70 s prior to  
203 Pb isotopic analysis to remove the gold coating and further minimize surface  
204 contamination. A  $300 \mu\text{m}$  aperture was used to project a 12-15 nA  $\text{O}_2^-$  primary beam with  
205 a slightly elliptical  $30 \mu\text{m}$  (long axis) spot on the surface of the sample. All analyses were  
206 conducted in multi-collector mode at a mass resolution of 4860 ( $M/\Delta M$ ), using an NMR  
207 field sensor in regulation mode to maintain the stability of the magnetic field. Lead  
208 isotopic ratios were measured in a multi-collector array of low noise ( $<0.03$  cps) ion-  
209 counting electron multipliers for 160 cycles with a count time of 10 s, resulting in a total  
210 collection time of 1600 s. Isotopic ratios were calculated as integrated means for all  
211 analyses. The largest potential source of inaccuracy is in the relative gain differences  
212 between ion counters, which is accounted for by bracketing unknown measurements with  
213 BCR-2G ( $\sim 11 \mu\text{g/g}$  Pb) and correcting isotopic measurements using the accepted values  
214 of this reference material (Woodhead and Hergt, 2000). External reproducibility for all  
215 measurements performed here in  $^{208}\text{Pb}/^{206}\text{Pb}$  and  $^{207}\text{Pb}/^{206}\text{Pb}$  is 0.3% and in  $^{208}\text{Pb}/^{204}\text{Pb}$ ,  
216  $^{207}\text{Pb}/^{204}\text{Pb}$ , and  $^{206}\text{Pb}/^{204}\text{Pb} = 0.9\%$ ,  $0.7\%$ , and  $1.0\%$ , respectively (all uncertainties  $2\sigma$ ).  
217 Lastly, for all of the Pb isotope modelling described below, the U decay constant  
218 recommendation of Steiger and Jäger (1977) and isotopic ratio of U ( $^{238}\text{U}/^{235}\text{U}$  of 137.88)  
219 were used.

220

#### 221 **4. Results**

222 Results from individual measurements of phases in the meteorites studied here are  
223 presented in Supplementary Table 1 and Supplementary Figure 1, while the x-y weighted

224 averages, which represent a single statistical population, for  $^{204}\text{Pb}/^{206}\text{Pb}$  vs.  $^{207}\text{Pb}/^{206}\text{Pb}$   
225 and  $^{208}\text{Pb}/^{206}\text{Pb}$  are presented in Table 1 and Figure 2. Maskelynite was the only phase  
226 analysed for all four enriched shergottites (Zagami, RBT 04262, LAR 12011, and KG  
227 002), the intermediate shergottite (ALH 77005), one depleted shergottite (LAR 12095),  
228 and ALH 84001 (this study and Bellucci et al., 2015a). Both sulfides and maskelynite  
229 were analysed in Tissint, since the sulfides had higher Pb concentrations and less  
230 radiogenic Pb than the maskelynite, they are assumed to represent the initial Pb in Tissint  
231 (Supplementary Figure 1). Unfortunately, the other depleted shergottite (LAR 12095)  
232 yielded no usable sulfide analyses due to isotopically heterogeneous time resolved  
233 spectra or overlapping SIMS spots with grain boundaries. The plagioclase in Nakhla did  
234 not experience enough shock pressure to be converted into maskelynite and was analysed  
235 here. The phases used to determine the initial Pb in Chassigny were three analyses of K-  
236 feldspar and a sulfide grain (Bellucci et al., 2016). A statistically identical population of  
237 the least radiogenic Pb isotope compositions were used to determine an x-y weighted  
238 average and any analyses outside of that statistically identical population were rejected  
239 (Supplementary Table 1). Similar to analyses of ALH 84001 (Bellucci et al., 2015a), it  
240 was impossible to determine an x-y weighted mean for  $^{204}\text{Pb}/^{206}\text{Pb}$  vs.  $^{208}\text{Pb}/^{206}\text{Pb}$  for  
241 Nakhla and Chassigny because the spread in the data generated an MSWD and  
242 probability of fit which were too large for a statistically identical population in two  
243 dimensions. As such, a one-dimensional weighted average of  $^{208}\text{Pb}/^{206}\text{Pb}$  compositions  
244 that correspond to the same analyses used in the calculation of the x-y weighted mean for  
245  $^{204}\text{Pb}/^{206}\text{Pb}$  vs.  $^{207}\text{Pb}/^{206}\text{Pb}$  were used to determine the initial Pb  $^{208}\text{Pb}/^{206}\text{Pb}$  composition  
246 for these two meteorites (Supplementary Figure 1). As reported with previous studies

247 using this method (Bellucci et al., 2015a), the initial Pb measurements reported here are  
248 the least radiogenic Pb analysed for each respective meteorite, contain no measurable U,  
249 and are therefore assumed to represent initial Pb for these samples (e.g., Bellucci et al.,  
250 2015a, 2016).

## 251 **5. Discussion**

### 252 *5.1 Shergottites*

253 Five of the shergottites studied have concordant ages in multiple isotopic systems  
254 and encompass all major groupings (depleted-intermediate-enriched). To produce  
255 accurate Pb model ages in agreement with those ages, a two-stage model can be  
256 constructed using previously established mantle chronology (after Stacey and Kramers,  
257 1975, Bellucci et al., 2015a). The Pb isotopic model used here starts at the time of Solar  
258 System formation at 4.567 Ga (Connelly et al., 2012) and begins with the Pb isotope  
259 composition of Canyon Diablo Troilite (CDT; Tatsumoto et al., 1973, Chen and  
260 Wasserburg, 1983). Since the estimate for the time of core formation on Mars is within  
261 error of that for Solar System formation (Kleine et al., 2004, 2009, Foley et al., 2005,  
262 Nimmo and Kleine, 2007, Dauphas and Pourmand, 2011) and the shergottite source  
263 reservoir experienced a mantle differentiation event at  $4.504^{+5.4}_{-.5.7}$  Ga (Borg et al.,  
264 2016), this two stage model encompasses two segments of Martian mantle history: 1)  
265 post-core formation and pre-silicate differentiation at 4.567 - 4.504 Ga and 2) post-  
266 silicate differentiation to time of crystallization for each meteorite (defined as the average  
267 of all radiogenic isotope system ages for an individual meteorite, Figure 1, Table 1). The  
268 accuracy of the model presented here is based on minimizing average  $\Delta_t$  where  $\Delta_t =$

269 crystallization age – Pb model age, and is presented in Figure 3. The age range and  
270 composition of shergottites for this study is expanded from that of Bellucci et al. (2015b)  
271 to include the depleted shergottite Tissint with a crystallization age of 574 Ma and the  
272 intermediate shergottite ALH 77005 with a crystallization age of 180 Ma (Figure 1). Over  
273 the five compositionally unique samples and ca. 600 Ma of crystallization history  
274 represented here, the average  $\Delta_t$  is minimized with a  $\mu_1$  (post-core formation, pre-silicate  
275 differentiation) of 1.8 (Figure 3). After the silicate differentiation event at 4.504 Ga, to  
276 achieve the correct Pb model ages, the source reservoirs require a  $\mu_2$  ranging from 1.4 –  
277 4.7 (Table 1, Figure 3).

278 Two of the shergottites analyzed here do not have external age constraints (KG  
279 002 and LAR 12095). Using the model obtained from all other shergottites, to achieve the  
280 initial Pb measured in KG 002, a model age of 360 Ma and a mantle  $\mu_2$ -value of 3.1 for  
281 both are required (Table 1). This model age is the oldest for the enriched shergottites yet  
282 studied, and the source mantle  $\mu$ -value is the lowest yet determined for an enriched  
283 shergottite. Due to the extremely low abundances of Pb and appropriately sized  
284 maskelynite, LAR 12095 has the biggest uncertainties associated with the estimation of  
285 initial Pb (Table 1, Figure 2). The initial Pb composition for LAR 12095 lies in a field  
286 that is more radiogenic in  $^{207}\text{Pb}/^{206}\text{Pb}$  than all of the models presented for this study. As  
287 such, a Pb-Pb model age for LAR 12095 would be a ‘future age’ and thus cannot be  
288 explicitly calculated for LAR 12095. Since there are no external age constraints for LAR  
289 12095, a source  $\mu$ -value cannot be explicitly calculated as opposed to the rest of the  
290 meteorites in this study. However, the source mantle  $\mu$ -value of 1.5 can be estimated

291 using only  $^{204}\text{Pb}/^{206}\text{Pb}$  for LAR 12095 and an age of 500 Ma, which is in broad  
292 agreement with its Lu-Hf and Sm-Nd systematics (Righter et al., 2015).

293

## 294 *5.2 Nakhla and Chassigny*

295 The shergottite model presented above cannot be used to calculate initial Pb  
296 model ages that are in agreement with the external age constraints of Nakhla and  
297 Chassigny. Therefore, the mantle from which these two meteorites originate must have a  
298 differentiation history that is fundamentally different to that of the shergottites. For the  
299 following discussion, it is assumed that these meteorites are derived from the same  
300 mantle source region (e.g., McCubbin et al., 2013). To construct the Pb isotopic model  
301 for the source region for these meteorites, the primordial Pb isotope composition was  
302 used (Canyon Diablo Troilite at 4.567 Ga) and since core differentiation was virtually  
303 simultaneous with accretion, it is ignored here. However, any secondary mantle  
304 differentiation event(s) lack other external age estimates, such as the 4.504 Ga age  
305 derived from the coupled Sm-Nd system determined for the shergottite source region  
306 (e.g., Borg et al., 2016). A simple approach is taken here and assumes a similar two-stage  
307 model to the shergottites. All of the potentially important events that reflect changes in  $\mu_1$   
308 (pre- silicate differentiation) and  $\mu_2$  (post- silicate differentiation) have been plotted in  
309 Figure 4. For a differentiation event occurring at 4.3 Ga or older, there exist no  $\mu_1$ -values  
310 that can be used to achieve the initial Pb compositions measured in Nakhla and  
311 Chassigny. Similarly, after 3.8 Ga, the generated curves do not have  $\mu_1$ -values that can be  
312 used to achieve the initial Pb compositions measured in these meteorites (shaded regions

313 in Figure 4). A median estimate between 4.3 and 3.8 Ga for the time of differentiation is  
314 at 4.1 Ga. This number has been chosen as an intermediate value between the boundary  
315 conditions. Choosing this value results in a pre-differentiation  $\mu_1$  of 0.75 and  
316 corresponding post differentiation  $\mu_2$  of 2.8 for Chassigny and 2.5 for Nakhla. This  $\mu_1$ -  
317 value and timing of differentiation is different from that of the shergottite source region  
318 of 1.8 (Figure 3). Since  $\mu_1$  is not consistent between meteorite groups, it explicitly  
319 implies that the early mantle differentiation history cannot be similar between both  
320 groups.

321         Since there are no external time constraints that can be used for comparison, these  
322 values for the differentiation time and subsequent  $\mu$ -values are speculative. However,  
323 some general statements can be made about the differentiation history for Chassigny and  
324 Nakhla. The isotopic composition needed at 4.1 Ga to produce the isotopic compositions  
325 of Nakhla and Chassigny is almost identical to that at 4.504 Ga needed to produce the  
326 isotopic compositions of the shergottites (Table 1, Figure 5). If the event at 4.504 Ga does  
327 represent the last stages of Martian accretion (e.g., Borg et al., 2016) and added primitive  
328 material to the Martian mantle, it would have mixed with any evolving Pb, thereby  
329 interfering with both the time of differentiation and  $\mu_1$ -value calculations here (Figure 5).  
330 Similarly, if material were added to the source region of the nakhlites and chassignites,  
331 any closed box modelling of all other isotopic systems would be explicitly affected (e.g.,  
332 Debaille et al., 2009). Any late additions of primitive material of CDT-like composition  
333 would have mixed with the evolving Pb and retarded the Pb growth, thus mathematically  
334 necessitating a decreased  $\mu_1$  value and a later time of differentiation. This is illustrated in  
335 Figure 5, whereby the growth trajectory of early Pb and mixing of early Pb with a

336 primitive reservoir (i.e., CDT) are geometrically similar but proceed in opposite  
337 directions. Therefore, if there were late additions of primitive material, it would have had  
338 the effect of retarding Pb evolution and decreasing the overall  $\mu$  in the source region  
339 through the addition of primordial Pb. This mixing phenomenon in Pb isotopes for early  
340 planetary evolution has also been recently considered to explain variations in the initial  
341 phases of Pb growth in the Earth-Moon system (Connelly and Bizzarro, 2016).

342

### 343 *5.3 Martian mantle differentiation history*

344 In addition to constraining the  $\mu$ -value of various Martian source reservoirs  
345 through time, initial Pb compositions can also be used to determine the time integrated  $\kappa$   
346 ratio of a planetary body. In  $^{208}\text{Pb}/^{206}\text{Pb}$  vs.  $^{204}\text{Pb}/^{206}\text{Pb}$ , initial Pb compositions of all  
347 samples measured here form a linear trend (Figures 2, 6). Using a Pb growth model  
348 beginning with assumed primordial CDT composition and the time of Solar System  
349 formation at 4.567 Ga, similar to the Pb growth models proposed earlier, most of the  
350 initial Pb compositions can be modelled with a  $\kappa$ -value of 3.6 (Figure 6), indicating that  
351 the Th/U value has not significantly fractionated during mantle differentiation events on  
352 Mars. Two meteorites lie outside of uncertainty of the modelled  $\kappa$ -value (Chassigny and  
353 the depleted shergottite LAR 12095) and may have been derived from mantle reservoirs  
354 with a slightly decreased Th/U. In addition, a  $\kappa$ -value of 3.6 is similar to that determined  
355 for the Earth, the Moon, and ordinary chondrites (Galer and O’Nions, 1985, Rocholl and  
356 Jochum, 1993, Snape et al., 2016).

357 For the first time, accurate Pb model ages with a corresponding source reservoir  
358  $\mu$ -value have been determined for all varieties of the shergottites, as well as Nakhla and  
359 Chassigny. Based on the models proposed here, a comparison between the source  
360 reservoir compositions for all other long-lived radiogenic isotope systems can now be  
361 inferred. When compared to the calculated mantle source  $\mu$ -values of 1.4-4.7 here, the  
362 source variables in  $^{87}\text{Sr}/^{86}\text{Sr}_i$ ,  $\gamma^{187}\text{Os}$ ,  $\epsilon^{176}\text{Hf}$ , and  $\epsilon^{143}\text{Nd}$  (given in Table 1) give strong  
363 linear correlations ( $r^2$  of 0.86, 0.95, 0.85, and 0.98 respectively, Figure 7). While the  
364 other source variables do not represent parent-daughter ratios like the  $\mu$ -values calculated  
365 here, they represent the time-integrated behavior of these radiogenic pairs. These linear  
366 correlations indicate that the major differentiation events of the Martian mantle affected  
367 all parent-daughter ratios of the shergottites and ALH 84001 at the same time, best  
368 determined for the time of the Martian silicate differentiation event at 4.504 Ga (Borg et  
369 al., 2016). It can be inferred that the mantle differentiation event that affected the parent-  
370 daughter ratios of radiogenic isotopic systems in the source reservoir of Nakhla and  
371 Chassigny must have behaved in a similar way.

372

#### 373 *5.4 Mars, other inner Solar System bodies, and implications for planetary* 374 *differentiation*

375 The original (post core formation, pre silicate differentiation) mantle source  
376 reservoir for Mars inferred from the shergottites had a  $\mu$ -value of 1.8. Since it is likely  
377 that the source region of Nakhla/Chassigny has experienced late addition/mixing and  
378 cannot record a pristine evolutionary history, the  $\mu$ -values for these meteorites are not



379 taken into account in the following discussion. A Martian initial  $\mu$ -value of 1.8 is not  
380 significantly elevated over ordinary and enstatite chondritic composition of  $\sim 1$  (e.g.,  
381 Tera, 1983, Göpel et al., 1994). Additionally, the most recent estimates for the ordinary  
382 chondrite materials that accreted to form the Earth indicate that these materials also had  
383 an initial  $\mu$ -value of 1.8 (Connelly and Bizzarro, 2016). Given the identical stable Cr  
384 isotopic compositions of ordinary, enstatite chondrites, the Moon, and the Earth (e.g.,  
385 Trinquier et al., 2009, Mougél et al., 2018), this  $\mu$ -value (1.8) seems likely to represent  
386 the primordial  $\mu$ -value of inner Solar System bodies.

387         If Mars accreted with a  $\mu$ -value of 1.8, like that proposed for the Earth and  
388 ordinary chondrites (e.g., Connelly and Bizzarro, 2016), and core formation occurred  
389 contemporaneously with planetary formation, it is very likely that core formation did not  
390 significantly affect the U/Pb value of silicate Mars (Martian mantle  $\mu$ -values of 1.4-4.7).  
391 This is in broad agreement with the low concentrations of Pb measured in iron meteorites  
392 (e.g., Tatsumoto et al., 1973) and similar observations for the very early Earth (e.g.,  
393 Connelly and Bizzarro, 2016). Thus, the increase in  $\mu$ -value for the intermediate and  
394 enriched shergottites must have occurred during the mantle differentiation event at 4.504  
395 Ga. It has been observed that the precipitation and fractionation of sulfides is able to  
396 elevate the  $\mu$ -value in an enriched residual source reservoir by a factor of around 4  
397 (Gaffney et al., 2007), which is in very good agreement with the present model for the  
398 intermediate-enriched shergottite source reservoirs with  $\mu$ -values of 3.1-4.7. This  
399 differentiation event at 4.504 Ga involving sulfides is also recorded in the complementary  
400 depleted shergottite reservoir with a  $\mu$ -value of 1.4-1.5.

401

## 402 **6. Conclusions**

403 In combination with previous studies, the initial Pb isotopic compositions of mantle-  
404 derived Martian meteorites including four enriched, one intermediate, and two depleted  
405 shergottites, Chassigny, and Nakhla have been measured in multiple analyses of  
406 maskelynite, plagioclase, K-feldspar and/or sulfide grains using SIMS. These data have  
407 been used to construct models of Pb isotopic evolution in both the shergottite source  
408 mantle reservoir(s) and the Nakhla/Chassignite source mantle reservoir(s), which, based  
409 on other isotopic systems, must have fundamentally distinct differentiation histories.  
410 These two separate models generate initial Pb model ages that are in complete agreement  
411 with the age constraints provided by all other radiogenic isotopic systems and provide an  
412 internally consistent chronology for the crystallization of Martian meteorites over 4 Ga of  
413 Martian history. However, the model for the differentiation history of the source reservoir  
414 of Nakhla/Chassigny is complicated by the evidence of likely late accretion.

415 The models constructed here have yielded  $\mu$ -values that have excellent linear  
416 correlations with other radiogenic isotopic source reservoir compositions ( $^{87}\text{Sr}/^{86}\text{Sr}_i$ ,  
417  $\gamma^{187}\text{Os}$ ,  $\varepsilon^{143}\text{Nd}$ , and  $\varepsilon^{176}\text{Hf}$ ), indicating a relatively simple differentiation history of the  
418 Martian mantle sampled by the shergottites. The model for the shergottites proposed here  
419 indicates that Mars accreted with an initial  $\mu$ -value of 1.8, which is in agreement with  
420 recent estimates for the early Earth and ordinary chondrites. Post accretion, the core  
421 formation had little to no affect on the bulk U/Pb value of Mars. At 4.504 Ga, the mantle  
422 experienced a differentiation event, which resulted in the formation of a depleted ( $\mu$ -  
423 value of 1.4-1.5), intermediate ( $\mu$ -value of 3.5) and enriched sources ( $\mu$ -values of 3.1-

424 4.7). Despite the fractionation events occurring in the U/Pb system,  $\kappa$  remained constant  
425 throughout Martian history with a value of 3.6, which is also in agreement with the Earth,  
426 the Moon, and chondrites.

427

## 428 **Acknowledgements**

429 The authors would like to acknowledge Kerstin Lindén for help preparing the  
430 samples. Dr. Ludovic Ferrière and the Natural History Museum Vienna are thanked for  
431 loaning the rock chip sample of Tissint used in this study. PAB acknowledges support  
432 from the Australian Research Council via their Australian Laureate Fellowship scheme.  
433 GKB acknowledges support from Curtin University via their Research Fellowship  
434 scheme and the Australian Research Council Discovery Grant number DP170102972.  
435 This work was funded by grants from the Knut and Alice Wallenberg Foundation  
436 (2012.0097) and the Swedish Research Council (VR 621-2012-4370) to MJW and AAN  
437 and VR grant (2016-03371) to J.J.B. Two anonymous reviewers are thanked for their  
438 comments that have improved the quality of this manuscript and Dr. Frederic Moynier is  
439 thanked for editorial handling. The NordSIMS ion microprobe facility operates as a  
440 Swedish-Icelandic infrastructure. This is NordSIMS publication #--.

441

## 442 **References**

- 443 Balta, J.B., Sanborn, M.E., Udry, A., Wadhwa, M. and McSween, H.Y. 2015. Petrology and trace element  
444 chemistry of Tissint, the newest shergottite fall. *Meteoritics & Planetary Science* 50, 63-85.  
445
- 446 Beard, B. L., Ludois, J. M., Lapen, T. J., & Johnson, C. M. (2013). Pre-4.0 billion year weathering on Mars  
447 constrained by Rb–Sr geochronology on meteorite ALH84001. *Earth and Planetary Science Letters*, 361,  
448 173-182.
- 449
- 450 Bellucci, J.J., Nemchin, A.A., Whitehouse, M.J., Snape, J.F., Bland, P. and Benedix, G.K. 2015a. The Pb  
451 isotopic evolution of the Martian mantle constrained by initial Pb in Martian meteorites. *Journal of*  
452 *Geophysical Research: Planets* 120, 2224-2240.

453  
454 Bellucci, J.J., Nemchin, A.A., Whitehouse, M.J., Humayun, M., Hewins, R. and Zanda, B. 2015b. Pb-  
455 isotopic evidence for an early, enriched crust on Mars. *Earth and Planetary Science Letters* 410, 34-41.  
456 DOI: 10.1016/j.epsl.2014.11.018

457 Bellucci, J.J., Nemchin, A.A., Whitehouse, M.J., Snape, J.F., Kielman, R.B., Bland, P.A. and Benedix,  
458 G.K. 2016. A Pb isotopic resolution to the Martian meteorite age paradox. *Earth and Planetary Science*  
459 *Letters* 433, 241-248. DOI: 10.1016/j.epsl.2015.11.004

460  
461 Blichert-Toft, J., Gleason, J.D., Télouk, P. and Albarède, F. 1999. The Lu-Hf isotope geochemistry of  
462 shergottites and the evolution of the Martian mantle-crust system. *Earth and Planetary Science Letters*. 173,  
463 25-39.

464  
465 Borg, L.E., Nyquist, L.E., Wiesmann, H. and Reese, Y. 2002. Constraints on the petrogenesis of Martian  
466 meteorites from the Rb-Sr and Sm-Nd isotopic systematics of the lherzolitic shergottites ALH 77005 and  
467 LEW 88516. *Geochimica et Cosmochimica Acta* 66, 2037-2053.

468  
469 Borg, L.E., Edmunson, J.E. and Asmerom, Y. 2005. Constraints on the U–Pb isotopic systematics of Mars  
470 inferred from a combined U–Pb, Rb–Sr, and Sm–Nd isotopic study of the Martian meteorite Zagami.  
471 *Geochim. Cosmochim. Acta* 69, 5819-5830.

472  
473 Borg, L.E. and Draper, D.S. 2003. A petrogenetic model for the origin and compositional variation of the  
474 Martian basaltic meteorites: *Meteoritics & Planetary Science*. 38, 1713-1731, doi:10.1111/j.1945-  
475 5100.2003.tb00011.x.

476  
477 Borg, L.E., Nyquist, L.E., Taylor, L.A., Wiesmann, H. and Shih, C.Y. 1997. Constraints on Martian  
478 differentiation processes from Rb-Sr and Sm-Nd isotopic analyses of the basaltic shergottite QUE 94201:  
479 *Geochimica et Cosmochimica Acta* 61, 4915-4931, doi:10.1016/S0016-7037(97)00276-7.

480  
481 Borg, L.E., Nyquist, L.E., Wiesmann, H., Shih, C.Y. and Reese, Y. 2003. The age of Dar al Gani 476 and  
482 the differentiation history of the Martian meteorites inferred from their radiogenic isotopic systematics:  
483 *Geochimica et Cosmochimica Acta* 67, 3519-3536, doi:10.1016/S0016-7037(03)00094-2

484  
485 Borg, L.E., Brennecka, G.A. and Symes, S.J.K. 2016. Accretion timescale and impact history of Mars  
486 deduced from the isotopic systematics of Martian meteorites. *Geochimica et Cosmochimica Acta*, 175,  
487 150-167.

488  
489 Brandon, A.D., Walker, R.J., Morgan, J.W. and Goles, G.G. 2000. Re-Os isotopic evidence for early  
490 differentiation of the Martian mantle. *Geochimica et Cosmochimica Acta*. 64, 4083-4095.

491  
492 Brandon, A.D., Puchtel, I.S., Walker, R.J., Day, J.M.D., Irving, A.J. and Taylor, L.A. 2012. Evolution of  
493 the Martian mantle inferred from the 187Re-187Os isotope and highly siderophile element abundance  
494 systematics of shergottite meteorites. *Geochimica et Cosmochimica Acta*. 76, 206-235.

495  
496 Brennecka, G.A., Borg, L.E. and Wadhwa, M. 2014. Insights into the Martian mantle: The age and  
497 isotopics of the meteorite fall Tissint. *Meteoritics & Planetary Science* 49, 412-418.

498  
499 Bouvier, A., Blichert-Toft, J., Vervoort, J.D., Gillet, P. and Albarède, F. 2008. The case for old basaltic  
shergottites. *Earth and Planetary Science Letters* 266, 105-124.

500  
501 Bouvier, A., Blichert-Toft, J. and Albarède, F. 2009. Martian meteorite chronology and the evolution of the  
502 interior of Mars. *Earth and Planetary Science Letters* 280, 285-295.

503  
504 Castle, N. and Herd, C.D.K. 2015. Petrogenesis of the LAR 12095/12240 Martian meteorite: Comparisons  
505 with Tissint and other depleted olivine-phyric shergottites. 46<sup>th</sup> Lunar and Planetary Science Conference  
Abstract #1975.

- 506  
507 Chen, J.H. and Wasserburg, G.J. 1983. The isotopic composition of silver and lead in two iron meteorites  
508 Cape York and Grant. *Geochimica et Cosmochimica Acta* 47, 1725-1737.
- 509  
510 Chen, J.H. and Wasserburg, G.J. 1986. Formation ages and evolution of Shergotty and its parent planet  
from U-Th-Pb systematics. *Geochimica et Cosmochimica Acta* 50, 955-968.
- 511  
512 Cohen, B. E., Mark, D. F., Cassata, W. S., Lee, M. R., Tomkinson, T., & Smith, C. L. (2017). Taking the  
pulse of Mars via dating of a plume-fed volcano. *Nature communications*, 8(1), 640.
- 513  
514 Connelly, J.N., Bizzarro, M., Krot, A.N., Nordlund, Å, Wielandt, D. and Ivanova, M.A. 2012. The absolute  
chronology and thermal processing of solids in the solar protoplanetary disk. *Science* 338. 651-655.
- 515  
516 Connelly, J.N. and Bizzarro, M. 2016. Lead isotope evidence for a young formation age of the Earth-Moon  
517 system. *Earth and Planetary Science Letters* 455, 36-43.
- 518  
519 Dauphas, N. and Pourmand, A. 2011. Hf-W-Th evidence for rapid growth of Mars and its status as a  
planetary embryo. *Nature* 473, 489-492.
- 520  
521 Debaille, V., Brandon, A.D., O'Neill, C., Yin, Q.-Z., and Jacobsen, B. 2009. Early Martian mantle overturn  
inferred from isotopic composition of Nakhlite meteorites. *Nature Geoscience*. 2, 548-552.
- 522  
523 Foley, C.N., Wadhwa, M., Borg, L.E., Janney, P.E., Hines, R. and Grove, T.L. 2005. The early  
524 differentiation history of Mars from  $^{182}\text{W}$ - $^{142}\text{Nd}$  isotope systematics in the SNC meteorites. *Geochimica et  
Cosmochimica Acta* 69, 4557-4571.
- 525  
526 Gaffney, A.M., Borg, L.E. and Connelly, J.N. 2007. Uranium lead isotope systematics of Mars inferred  
from the basaltic shergottite QUE 94201. *Geochimica et Cosmochimica Acta* 71, 5016-5031.
- 527  
528 Gale, N.H., Arden, J.W. and Hutchison, R. 1975. The chronology of the Nakhla achondritic meteorite.  
529 *Earth and Planetary Science Letters* 26, 195-206.
- 530  
531 Galer, S.J.G. and O'Nions, R.K. 1985. Residence time of thorium, uranium and lead in the mantle with  
implications for mantle convection. *Nature* 316, 778-782.
- 532  
533 Göpel, C., Manhès, G. and Allegre, C.J. 1985. U-Pb systematics in iron meteorites: Uniformity of  
534 primordial lead. *Geochimica et Cosmochimica Acta*. 49, 1681-1695.
- 535  
536 Grosshans, T.E., Lapen, T.J., Andreasen, R. and Irving, A.J. 2013. Lu-Hf and Sm-Nd ages and source  
compositions for depleted shergottite Tissint. 44<sup>th</sup> Lunar and Planetary Science Conference, Abstract #2872.
- 537  
538 Hart, S.R., Hauri, E.H., Oschmann, L.A. and Whitehead, J.A. 1992. Mantle plumes and entrainment:  
Isotopic evidence. *Science* 256, 517-520.
- 539  
540 Harvey, R.P. and McSween, H.Y. 1992. Petrogenesis of the Nakhlite meteorites: Evidence from cumulate  
mineral zoning. *Geochimica et Cosmochimica Acta* 56, 1655-1663.
- 541  
542 Kleine, T., Mezger, K., Münker, C., Palme, H. and Bischoff, A. 2004.  $^{182}\text{Hf}$ - $^{182}\text{W}$  isotope systematics of  
543 chondrites, eucrites and Martian meteorites: Chronology of core formation and early mantle differentiation  
in Vesta and Mars. *Geochimica et Cosmochimica Acta* 68, 2935-2946.
- 544  
545 Kleine, T., Touboul, M., Bourdon, B., Nimmo, F., Mezger, K., Palme, H., Jaconsen, S.B., Yin, Q.-Z. and  
546 Halliday, A.N. 2009. Hf-W chronology of the accretion and early evolution of asteroids and terrestrial  
planets. *Geochimica et Cosmochimica Acta* 73, 5150-5188.

- 547 Kruijer, T. S., Kleine, T., Borg, L. E., Brennecka, G. A., Irving, A. J., Bischoff, A., & Agee, C. B. (2017).  
548 The early differentiation of Mars inferred from Hf–W chronometry. *Earth and Planetary Science Letters*,  
549 474, 345-354.
- 550 Lapen, T.J., Brandon, A.D., Beard, B.L., Peslier, A.H., Lee, C-T.A. and Dalton, H.A. 2008. Lu-Hf age and  
551 isotopic systematics of the olivine-phyric shergottite RBT-04262 and implications for the source of  
552 enriched shergottites. 39<sup>th</sup> Lunar and Planetary Science Conference, XXXIX. Abstract #2073.  
553
- 554 Lapen, T.J., Righter, M., Brandon, A.D., Debaille, V., Beard, B.L., Shafer, J.T. and Preslier, A.H. 2010. A  
555 younger age for ALH 84001 and its geochemical link to shergottite sources in Mars. *Science* 328, 347-351.  
556
- 557 Llorca, J., Roszjar, J., Cartwright, J.A., Bischoff, A., Ott, U., Pack, A., Merchel, S., Rugel, G., Fimiani, L.,  
558 Ludwig, P, Casado, J.V. and Allepuz, D. 2013. The Ksar Ghilane 002 shergottite - The 100<sup>th</sup> registered  
559 Martian meteorite fragment. *Meteoritics & Planetary Science* 48, 493-513.
- 560 McSween, H.Y.Jr., Taylor, L.A. and Stolper, E.M. 1979. Allan Hills 77005: A new meteorite type found in  
561 Antarctica. *Science* 204, 1201-1203.
- 562 McCubbin, F.M., Elardo, S.M., Shearer, C.K., Smirnov, A., Hauri, E.H. and Draper, D.S. 2013. A  
563 petrogenetic model for the comagmatic origin of chassignites and nakhlites: Inferences from chlorine-rich  
564 minerals, petrology, and geochemistry *Meteoritics & Planetary Science* 48, 819-853.
- 565 Mezger, K., Debaille, V. and Kleine, T. 2013. Core formation and mantle differentiation on Mars. *Space*  
566 *Science Reviews* 174, 27-48.
- 567 Misawa, K., Shih, C-Y., Reese, Y., Bogard, D.D. and Nyquist, L.E. 2006. Rb-Sr, Sm-Nd, and Ar-Ar  
568 isotopic systematics of Martian dunite Chassigny. *Earth and Planetary Science Letters* 246, 90-101.  
569
- 570 Moriwaki, R., Usui, T., Simon, J.I., Jones, J.H., Yokoyama, T. and Tobita, M. 2017. Coupled Pb isotopic  
571 and trace element systematics of the Tissint meteorite: Geochemical signatures of the depleted shergottite  
572 source mantle. *Earth and Planetary Science Letters* 474, 180-189.  
573
- 574 Mougél, B., Moynier, F., & Göpel, C. (2018). Chromium isotopic homogeneity between the Moon, the  
575 Earth, and enstatite chondrites. *Earth and Planetary Science Letters*, 481, 1-8.  
576
- 577 Nakamura, N., Unruh, D.M., Tatsumoto, M. and Hutchison, R. 1982. Origin and evolution of the Nakhla  
578 meteorite inferred from the Sm-Nd and U-Pb systematics and REE, Ba, Sr, Rb abundances. *Geochimica et*  
579 *Cosmochimica Acta* 46, 1555-1573.  
580
- 581 Nimmo, F. and Kleine, T. 2007. How rapidly did Mars accrete? Uncertainties in the Hf-W timing of core  
582 formation. *Icarus* 191, 497-504.
- 583 Papanastassiou, D.A. and Wasserburg, G.J. 1974. Evidence for late formation and young metamorphism in  
584 the achondrite Nakhla. *Geophysical Research Letters* 1, 23-26.  
585
- 586 Rocholl, A. and Jochum, K.P. 1993. Th, U and other trace elements in carbonaceous chondrites:  
587 Implications for the terrestrial and solar-system Th/U ratios. *Earth and Planetary Science Letters* 117, 265-  
588 278.
- 589 Righter, M., Andreasen, R. and Lapen, T.J. 2015. Lu-Hf and Sm-Nd systematics of Martian meteorites  
590 Larkman Nunatak 12011 and 12095. 46<sup>th</sup> Lunar and Planetary Science Conference, Abstract #2889.  
591
- 592 Shafer, J.T., Brandon, A.D., Lapen, T.J., Righter, M., Peslier, A.H. and Beard, B.L. 2010. Trace element  
593 systematics and <sup>147</sup>Sm-<sup>143</sup>Nd and <sup>176</sup>Lu-<sup>176</sup>Hf ages of Larkman Nunatak 06319: Closed-system fractional  
594 crystallization of an enriched shergottite magma. *Geochimica et Cosmochimica Acta* 74, 7307-7328.

595  
596 Shih, C-Y., Nyquist, L.A. and Reese, Y. 2009. Rb-Sr and Sm-Nd studies of olivine-pyric shergottites RBT  
597 04262 and LAR 06319: Isotopic evidence for relationship to enriched basaltic shergottites. 40<sup>th</sup> Lunar and  
598 Planetary Science Conference, Abstract #1360.  
599  
600 Snape, J.F., Nemchin, A.A., Bellucci, J.J., Whitehouse, M.J., Tartèse, R., Barnes, J.J., Anand, M., Crawford,  
601 I.A. and Joy, K.H. 2016. Lunar basalt chronology, mantle differentiation and implications for determining  
602 the age of the Moon. *Earth and Planetary Science Letters* 451, 149-158.

603 Stacey, J.S. and Kramers, J.D. 1975. Approximation of terrestrial lead isotope evolution by a two-stage  
604 model. *Earth and Planetary Science Letters* 26, 207-221.  
605  
606 Steiger, R.H. and Jäger, E. 1977. Subcommittee on geochronology: Convention on the use of decay  
607 constants in geo- and cosmochronology. *Earth and Planetary Science Letters* 36(3), 359-362.

608 Tatsumoto, M., Knight, R.J. and Allegre, C.J. 1973. Time differences in the formation of meteorites as  
609 determined from the ratio of Lead-207 to Lead-206. *Science* 180, 1279-1283.

610 Tera, F. 1983. U-Th-Pb in chondrites-evidence of elemental mobilities and the singularity of primordial Pb.  
611 *Earth and Planetary Science Letters* 63, 147-166.  
612  
613 Trinquier, A., Elliott, T., Ulfbeck, D., Coath, C., Krot, A.N. and Bizzarro, M. 2009. Origin of  
614 nucleosynthetic isotope heterogeneity in the solar protoplanetary disk. *Science* 324, 374-376.  
615  
616 Whitehouse, M.J., Kamber, B.S., Fedo, C.M. and Lepland, A. 2005. Integrated Pb- and S- isotope  
617 investigation of sulphide minerals from the early Archean of southwest Greenland. *Chemical Geology*, 222,  
618 112-131.  
619  
620 Woodhead, J.D. and Hergt, J.M. 2000. Pb-isotope analyses of USGS reference materials. *Geostandards and*  
621 *Geoanalytical Research* 24, 33-38.  
622  
623 Zartman, R.E. and Haines, S.M. 1988. The plumbotectonic model for Pb isotopic systematics among major  
624 terrestrial reservoirs - A case for bi-directional transport. *Geochimica et Cosmochimica Acta* 52, 1327-  
625 1339.

626  
627  
628  
629  
630  
631  
632  
633  
634  
635  
636  
637  
638  
639  
640  
641  
642

643  
644  
645

## Figures

646 **Figure 1.** Weighted averages for the ages of the meteorites studied here. All age  
647 constraints are from isotopic systems in the legend on the figure. References for each  
648 meteorite as follows: RBT 04262: Lapen et al. (2008) and Shih et al. (2009), Zagami:  
649 Borg et al. (2005); LAR 12011: Shafer et al. (2010); ALH 77005: Borg et al. (2002);  
650 Tissint: Brennecka et al. (2014); Chassigny: Misawa et al. (2006); Nakhla: Cohen et al.,  
651 (2017), Gale et al. (1975), Nakumurua et al. (1982), Papanastassiou and Wasserburg  
652 (1974).

653

654 **Figure 2.** Initial Pb compositions for ten Martian meteorites investigated. Each symbol is  
655 representative of an x-y weighted average of several maskelynite, plagioclase, K-  
656 feldspar, or sulfide analyses from each meteorite (See Supplementary Figure 1 and  
657 Bellucci et al., 2015a). Included in this diagram are lines corresponding to shergottite  
658 model time (S.m.t., after Figure 3) that correspond to all  $\mu$ -values at a given time at time  
659 at 4090 Ma, 500 Ma, and 0 Ma (S.m.t: solid lines). Similarly, the dashed line illustrates a  
660 1400 Ma age determined using the Chassigny and Nakhla model (Chassigny and Nakhla  
661 model time: C.N.m.t.) described in Figure 4.

662

663 **Figure 3.** A two-stage Pb isotopic model for the shergottites studied here with concordant  
664 ages in other isotopic systems (Figure 1). The model assumes a silicate differentiation  
665 event at 4.504 Ga (Borg et al., 2016), minimizes the average  $\Delta_t$  (difference between  
666 initial Pb model age-concordant age), and determines  $\mu$ -values after core formation and



667 pre 4.504 Ga ( $\mu_1$ ) and post 4.504 Ga ( $\mu_2$ ). Gray bands represent  $2\sigma$  uncertainty estimates  
668 on the average  $\Delta_t$  of Pb model ages.

669

670 **Figure 4.** A two-stage Pb isotope model for the Nakhla and Chassigny. Since there is no  
671 information on the differentiation history of the Martian mantle that led to these mantle  
672 reservoirs, various arbitrary timing for multiple differentiation events are used. Boundary  
673 conditions exist where average  $\Delta_t=0$  cannot have occurred before 4.3 and after 3.8 Ga  
674 (grey shaded regions). The dashed line at  $\mu_1$  of 0.75 corresponds to our estimate of the  
675 median mathematical solution at 4.1 Ga.

676

677 **Figure 5.** Pb growth from (primordial) CDT to 4.504 Ga (black curve) and mixing line  
678 between evolved Pb and CDT composition (red dashed curve). The trajectory of the Pb  
679 growth from 4.567 Ga to 4.504 Ga and mixing in Pb-Pb diagrams are linear, but opposite.  
680 Therefore, any additions of primitive Pb composition would have apparently retarded any  
681 Pb growth but kept it on the same geometrical trajectory. This retardation would dictate  
682 mathematical requirements of a lower  $\mu_1$  and a later time of differentiation presented,  
683 which was calculated in Figure 4.

684

685 **Figure 6.** A time integrated  $\kappa$  ( $^{232}\text{Th}/^{238}\text{U}$ ) value from 4.567 Ga to present of 3.6 is  
686 calculated in  $^{204}\text{Pb}/^{206}\text{Pb}$  vs.  $^{208}\text{Pb}/^{206}\text{Pb}$  for all investigated samples. The linearity seen  
687 between samples in this figure indicates that there has been limited fractionation between  
688 U and Th in the Martian mantle, as represented by the range of sample material analyzed  
689 here, through geologic time.

690

691 **Figure 7.** Mantle source  $\mu$ -values vs. other the source values for other long-lived  
692 radiogenic parameters including  $^{87}\text{Sr}/^{86}\text{Sr}_i$ ,  $\gamma^{188}\text{Os}$ ,  $\varepsilon^{176}\text{Hf}$ , and  $\varepsilon^{143}\text{Nd}$ . These parameters  
693 reflect the time-integrated behavior of the parent/daughter ratios throughout Martian  
694 history, similar to the  $\mu$ -values calculated here. The  $\text{Sr}_i$  value for ALH84001 is plotted  
695 but was excluded from the linear regression due to its possible mixing with an elevated  
696 Rb/Sr source during its formation or analysis (Beard et al., 2013). Excellent linear  
697 correlations indicate relatively simple parent-daughter fractionations during mantle  
698 differentiation events. References for each value are presented in Table 1.

699

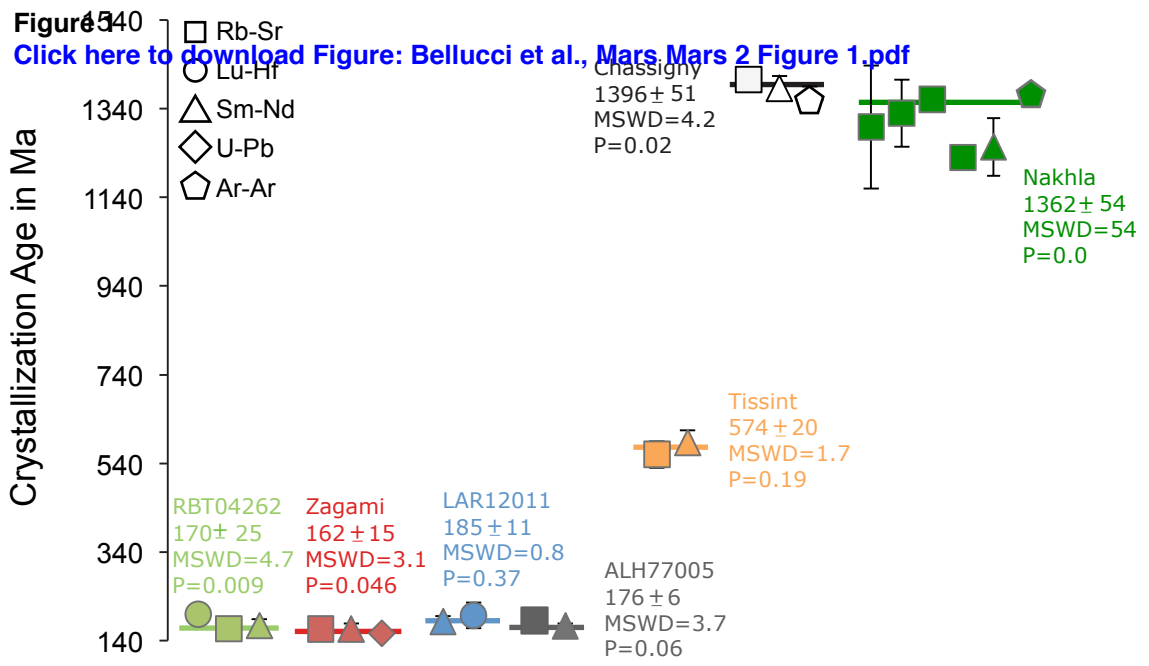
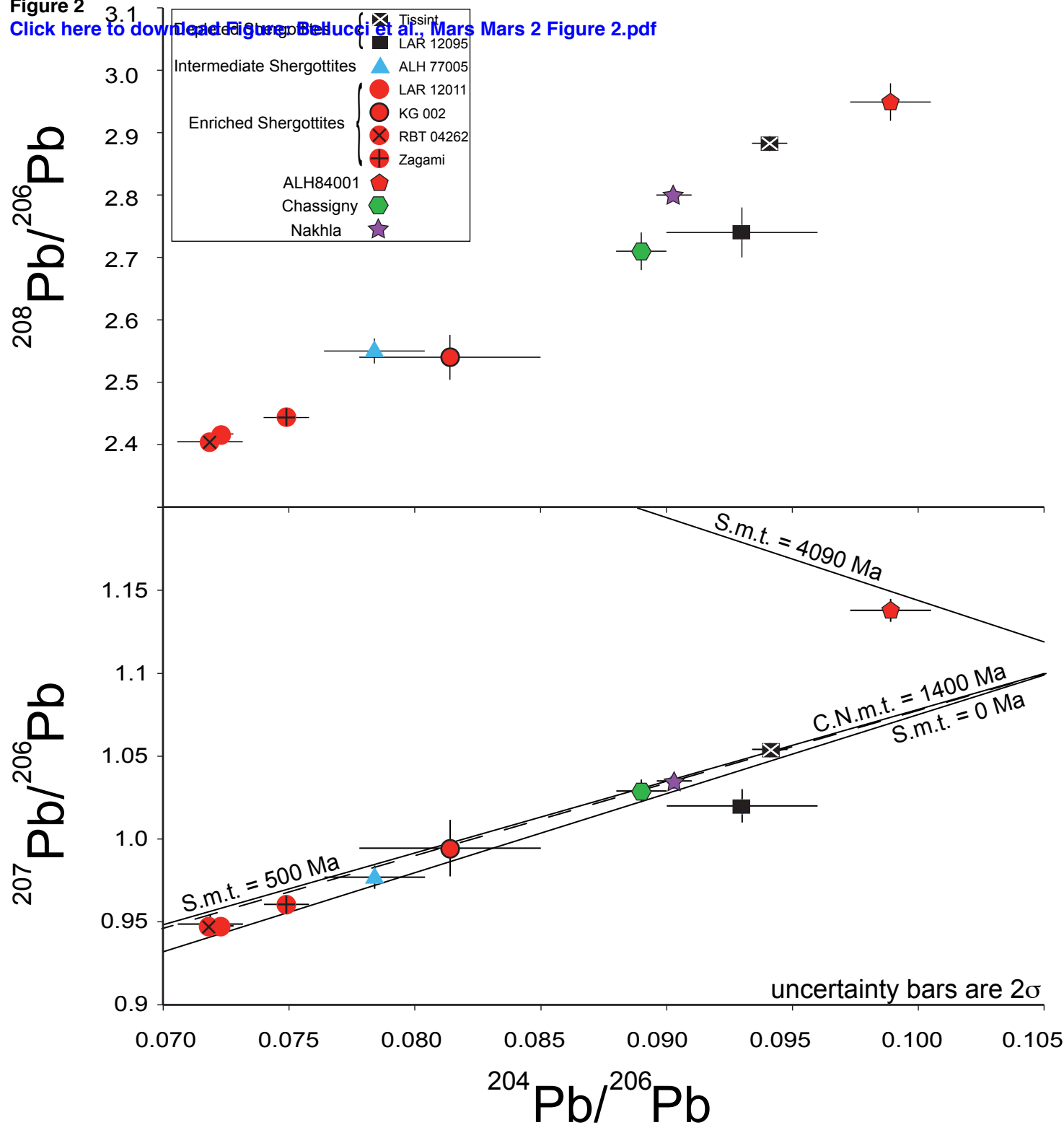


Figure 2  
Click here to download Figure 2: Belucci et al., Mars Mars 2 Figure 2.pdf



**Figure 3**

[Click here to download Figure: Bellucci et al., Mars Mars 2 Figure 3.pdf](#)

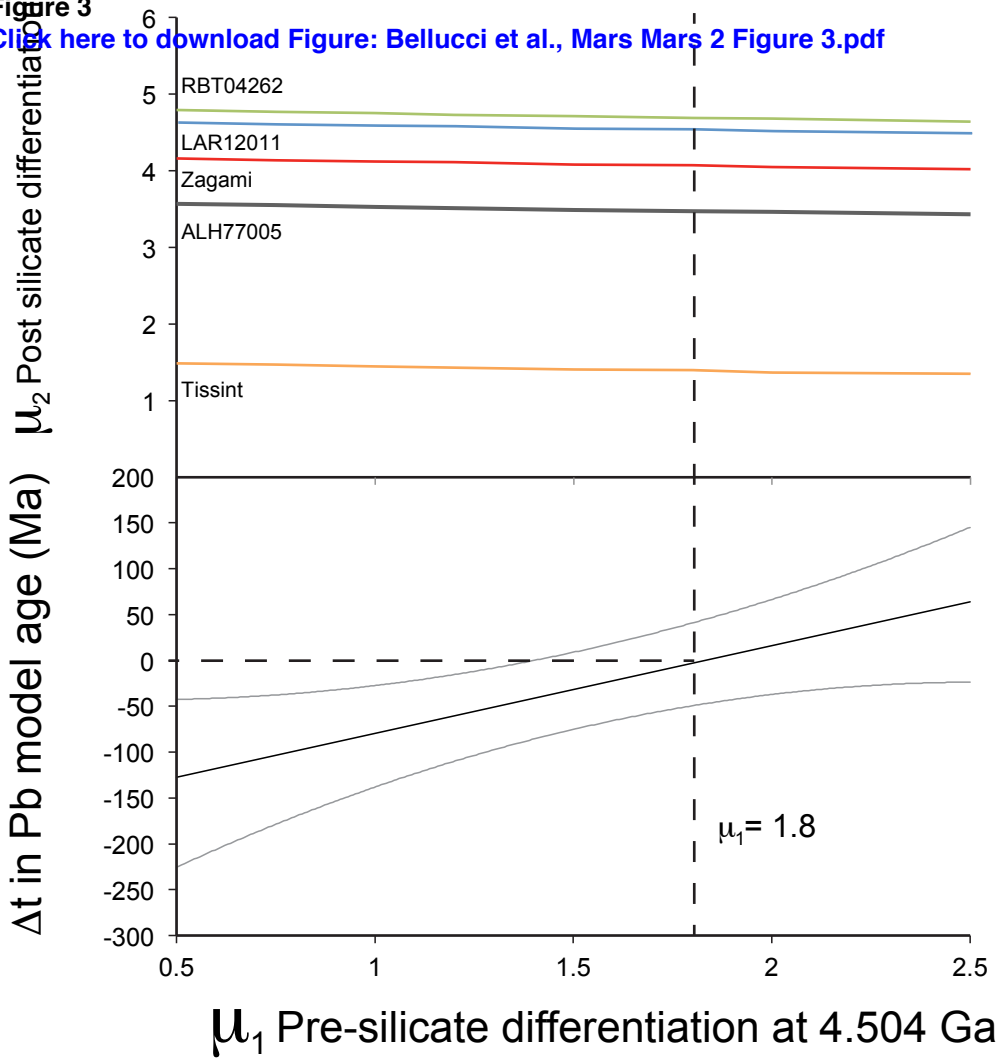


Figure 4

[Click here to download Figure: Bellucci et al., Mars Mars 2 Figure 4.pdf](#)

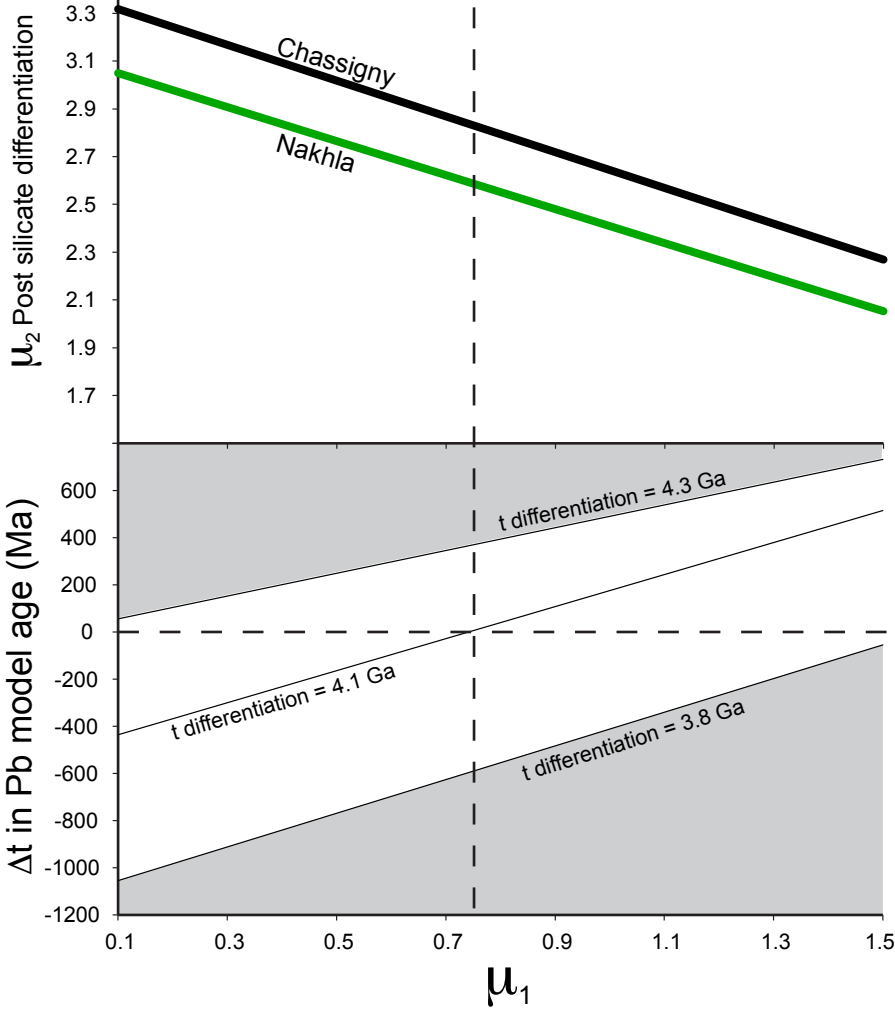
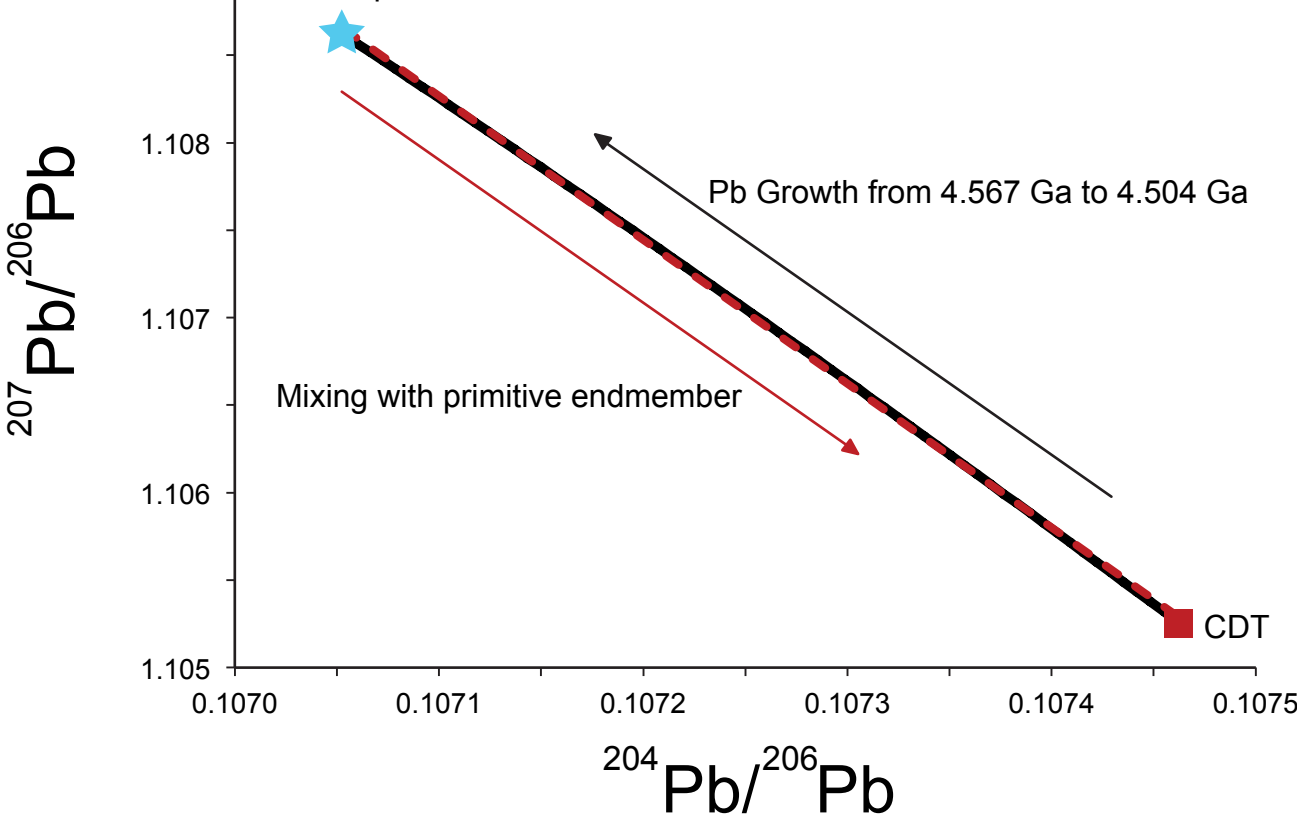
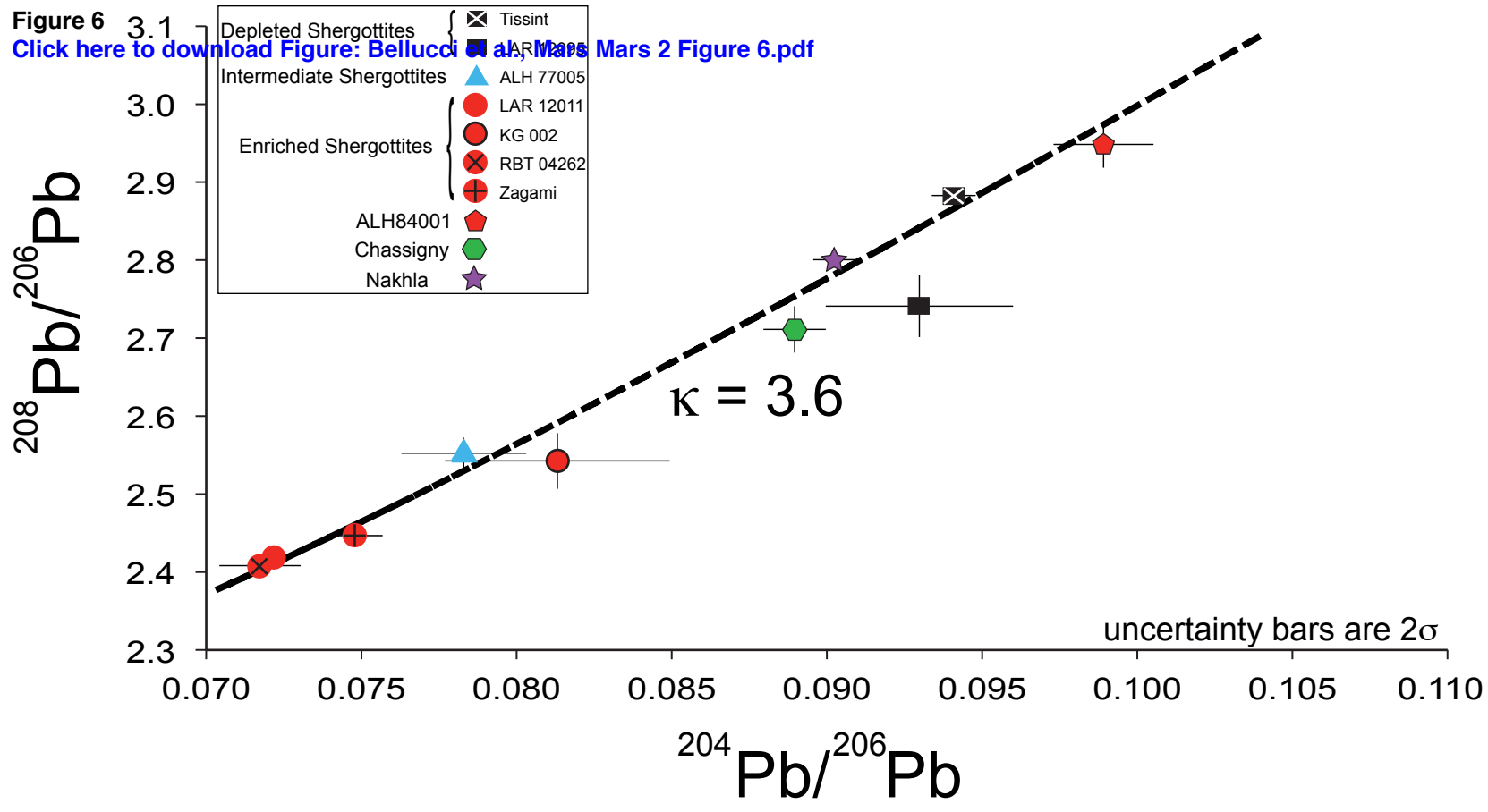


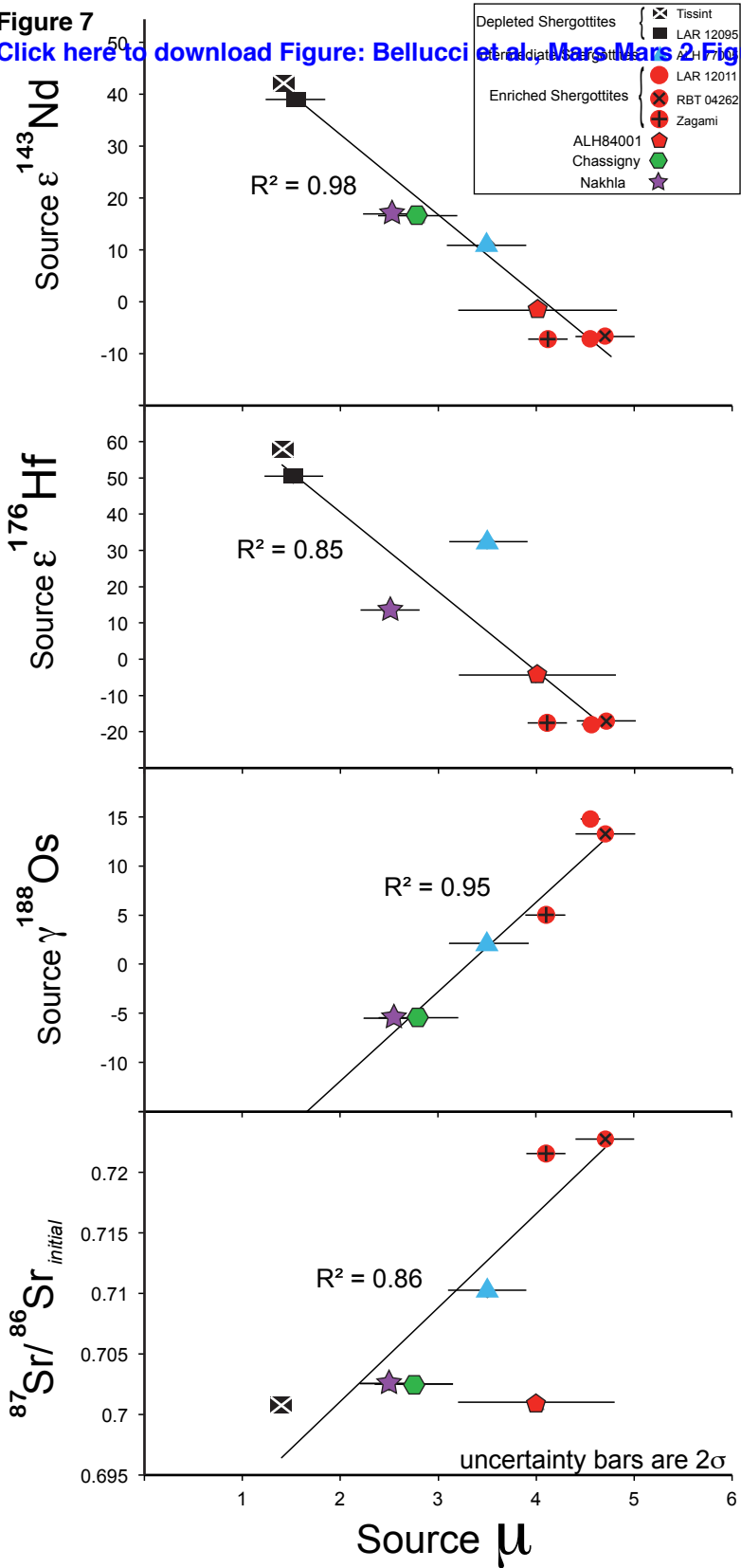
Figure 5

[Click here to download Pb composition at 4.504 Ga Mars 2 Figure 5.pdf](#)







**Figure 7**[Click here to download Figure: Bellucci et al., Mars Mars 2 Fig](#)

**Table 1**  
[Click here to download Table: Bellucci et al., 2017 Mars 2 Table 1.xlsx](#)

**Table 1. Initial Pb isotopic compositions, model ages, and source compositions**

Sample	Type	$^{208}\text{Pb}/^{206}\text{Pb}$	2	$^{207}\text{Pb}/^{206}\text{Pb}$	2	$^{206}\text{Pb}/^{206}\text{Pb}$	2	n	Crystallization Age <sup>1</sup> in Ma	Pb Model Age in Ma	2	t <sup>*</sup>	1	2	2	$^{176}\text{Hf}$ Source	$^{143}\text{Nd}$ Source	$^{187}\text{Os}$ Source
RBT 04261 <sup>2</sup>	Enriched	0.0719	0.0013	0.949	0.006	2.405	0.011	14	170	240	180	-70	1.8	4.7	0.3	-17 <sup>a</sup>	-6.7 <sup>d</sup>	13.2 <sup>e</sup>
LAR 12011 <sup>2</sup>	Enriched	0.0723	0.0005	0.948	0.002	2.417	0.006	37	185	150	76	35	1.8	4.6	0.1	-18 <sup>l</sup>	-7.2 <sup>l</sup>	14.7 <sup>c</sup>
Zagami <sup>2</sup>	Enriched	0.0749	0.0009	0.961	0.004	2.443	0.007	20	165	170	158	-5	1.8	4.1	0.2	-17.6 <sup>g</sup>	-7.2 <sup>d</sup>	5 <sup>f</sup>
KG 002	Enriched	0.0814	0.0036	0.995	0.017	2.540	0.036	20	NA	360	802	NA	1.8	3.1	0.8	NA	NA	NA
ALH 77055	Intermediate	0.0784	0.0020	0.977	0.007	2.550	0.020	10	176	180	302	-4	1.8	3.5	0.4	32.4 <sup>a</sup>	11.1 <sup>b</sup>	2.1 <sup>f</sup>
LAR 12095	Depleted	0.093	0.003	1.02	0.01	2.74	0.04	18	NA	NA	NA	NA	1.8	1.5	0.3	50.4 <sup>l</sup>	39 <sup>l</sup>	NA
Tissint	Depleted	0.0941	0.0007	1.054	0.003	2.883	0.008	5	574	570	213	4	1.8	1.4	0.1	58 <sup>h</sup>	42 <sup>h</sup>	NA
ALH 84001 <sup>2</sup>		0.0989	0.0016	1.138	0.007	2.949	0.030	18	4090 <sup>k,2</sup>	3850	170	240	1.8	4.0	0.8	-4.37 <sup>j</sup>	-1.6 <sup>f</sup>	NA
Composition of the Shergottite/ALH84001 source Mantle		0.107		1.11		3.16												
Chassigny <sup>3</sup>		0.0890	0.0010	1.029	0.007	2.710	0.030	4	1396	1400	256	-4	0.75	2.8	0.4	NA	16.6 <sup>m</sup>	-5.46 <sup>n</sup>
Nakhla		0.0903	0.0007	1.035	0.003	2.800	0.010	13	1362	1380	214	-18	0.75	2.5	0.3	13.5 <sup>n</sup>	16.9 <sup>h</sup>	-5.5 <sup>n</sup>
Nakhla/Chassigny Source at 4.1 Ga		0.106		1.11		3.14												

a) Blichert-Toft et al., 1999 b) Borg et al., 2002, c) Brandon et al., 2012, d) Borg et al., 2005, e) Brandon et al., 2000, f) Lapen et al., 2010, g) Brennecka et al., 2014, h) Grosshans et al., 2013, i) Righter et al., 2015, j) Shafer et al., 2010, k) Lapen et al., 2008, l) Shih et al., 2009, m) Misawa et al., 2005, n) Debaille et al., 2009, o) Beard et al., 2013, p) Gale et al., 2015, q) Bellucci et al., 2015, r) Bellucci et al., 2016

1) See Figure 1

2) Pb isotope values from Bellucci et al., 2015a

3) Pb isotope values from Bellucci et al., 2016

**Supplementary material for online publication only**

[Click here to download Supplementary material for online publication only: Bellucci et al., 2016 Mars Mantle Pb Supplementary](#)

**Supplementary material for online publication only**

**[Click here to download Supplementary material for online publication only: Bellucci et al., 2017 Mars 2 SuppTable 1.xlsx](#)**